

Learning Terrain-Aware Whole-Body Control for Perceptive Legged Loco-Manipulation

Sikai Guo, Yudong Zhong, Guoyang Zhao, Botao Dang, Zhihai Bi, Jun Ma

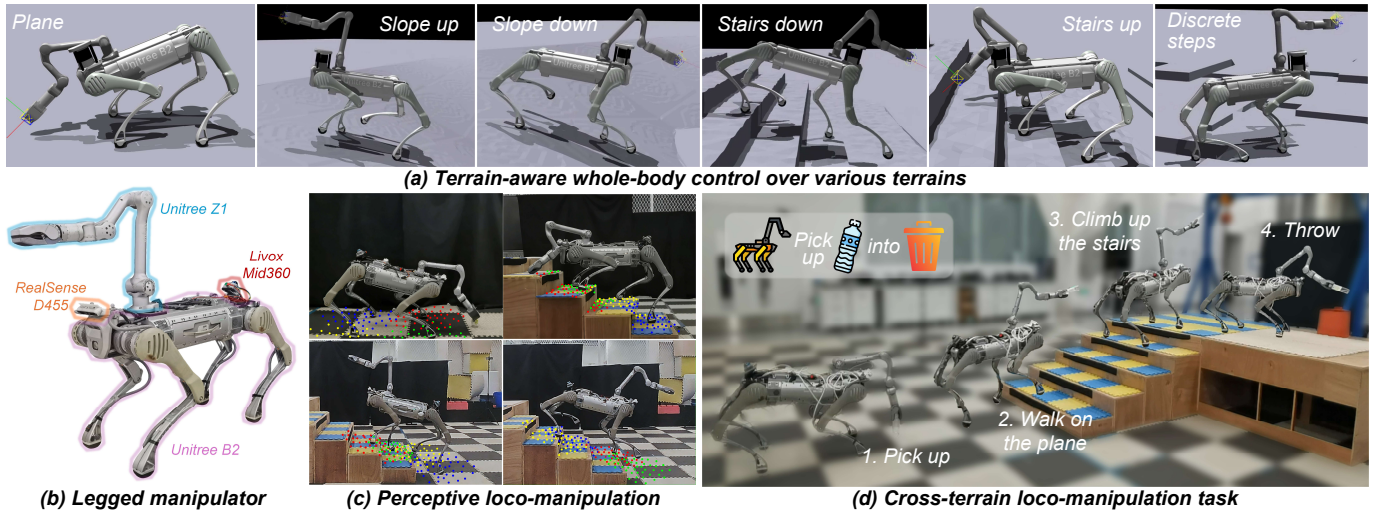


Fig. 1: TA-WBC is a terrain-aware whole-body controller for perceptive legged loco-manipulation over diverse challenging terrains, including slopes, stairs, and steps. With terrain exteroception, it enables legged manipulators to actuate whole-body joints for expanding workspace, while maintaining collision-free cross-terrain traversal capabilities.

Abstract—Legged manipulators integrate exceptional terrain adaptability along with mobile manipulation capabilities, which make them highly promising for deployment in human-centric environments. By coordinating the control of both legs and arms, a whole-body controller can significantly expand the operational workspace of legged manipulators. However, many existing whole-body controllers primarily depend on proprioception and do not incorporate the critical exteroception required for effective terrain topology perception. This limitation can hinder their ability to adapt to varying environmental conditions and navigate complex terrains effectively. In this paper, we introduce TA-WBC, a terrain-aware whole-body control framework for legged manipulators, which features a novel RL-based unified policy tailored to whole-body loco-manipulation tasks in various terrains. Specifically, we employ a hybrid exteroception encoder to extract terrain features, providing an essential basis for the robot to proactively adapt posture and footholds. Furthermore, to facilitate stable cross-terrain loco-manipulation, we propose a novel end-effector sampling method based on the foot contact plane, decoupling manipulation target from base fluctuations. Moreover, a dual-policy distillation module is introduced to integrate expansive whole-body motion with terrain adaptability without catastrophic forgetting. The simulation and real-world experiments validate the robustness of our proposed controller, which leads to a larger reachable space, less tracking error, and reduced unexpected stumbles. This unified policy highlights the promising capabilities of legged manipulators in performing loco-manipulation tasks across complex terrains.

I. INTRODUCTION

Over the past decade, mobile manipulation systems have achieved significant advancements, with a remarkable transi-

tion from confined industrial environments to human-centric settings [1], [2]. A typical mobile manipulator generally comprises a mobile base and an onboard robotic arm, allowing the system to move its base while simultaneously performing manipulation tasks with the end effector, thereby extending its effective workspace. While there have been some rather promising preliminary works on wheeled manipulators in structured spaces, their mobility is fundamentally constrained to planar or flat surfaces, limiting their utility in complex scenarios such as disaster response, construction sites, or multi-level residential areas. Legged manipulators, particularly quadruped robots equipped with robotic arms, offer a compelling solution [3], [4]. Essentially, they not only have the inherent capability of traversing unstructured terrains, but also can leverage the redundancy of the floating base to extend the reachable workspace. For instance, they can bend their front legs to reach the ground with the end-effector, or elevate the front body to grasp higher objects[5].

Despite this potential, achieving coordinated whole-body control (WBC) for legged manipulators remains inherently challenging. The core difficulty lies in the complex whole-body dynamics and the coupling between the high degree-of-freedom (DoF) system and high-accuracy manipulation tasks. Traditional model-based methods for WBC, such as model predictive control (MPC) [3], [6], or hierarchical quadratic programming (QP) [7], [8], rely on precise dynamic modeling and are often computationally intensive. This feature makes them susceptible to unmodeled external disturbances, and unable to stay robust in unstructured environments. Conversely, reinforcement learning (RL) has recently emerged as a powerful alternative for developing robust legged-manipulation controllers. By introducing regularized online adaptation [4]

Sikai Guo, Yudong Zhong, Guoyang Zhao, Botao Dang, Zhihai Bi, and Jun Ma are with the Robotics and Autonomous Systems Thrust, The Hong Kong University of Science and Technology (Guangzhou), Guangzhou 511453, China.

and teacher-student training framework [9], the RL-based controller bridges the sim-to-real gap, demonstrating superior disturbance rejection and enhanced whole-body coordination [10], [11], all without requiring complex dynamic modeling.

However, most existing whole-body controllers for legged manipulation are developed under the assumption of flat and quasi-horizontal terrain. They are typically reliant on proprioception solely, enabling locomotion without external environmental perception, and treating terrain irregularities as unmodeled disturbances that are addressed in a reactive manner [12]. Although recent works like PILOT [13] achieves perceptive cross-terrain loco-manipulation for humanoid robots, perceptive whole-body control remains particularly challenging for quadrupedal manipulators, since they lack direct human demonstrations for their non-anthropomorphic morphology. Overall, there are three main challenges when the legged manipulators are executing loco-manipulation tasks in unstructured environments. First, when traversing terrains like stairs or steps, a blind robot has to first make unexpected contact with the obstacles to sense the disturbance, inevitably causing sudden pose perturbation in the floating base and compromising onboard end-effector tracking accuracy. Second, the training of existing works relies on end-effector goal sampling strategies restricted to flat terrains, which fails to achieve continuous stability of the end-effector in cross-terrain loco-manipulation tasks due to base pose and height variations. Third, although decoupling perceptive locomotion and blind whole-body control into separate policies can be feasible in certain cases [14], this solution requires a complex high-level decision module or manual operation for policy switching. Generally, a unified controller can address this challenge, but it is difficult to train a single policy integrating whole-body coordination ability with multi-terrain adaptability.

To solve the above open challenges, we present the Terrain-Aware Whole-Body Control (TA-WBC), a unified end-to-end low-level controller for perceptive legged loco-manipulation over various terrains, as shown in Fig. 1. Specifically, it incorporates a hybrid exteroception encoder of convolutional networks and multilayer perceptron (MLP), capable of extracting environmental geometric features around feet to avoid undesired foot contact while traversing terrains. Furthermore, to facilitate end-effector tracking accuracy in cross-terrain loco-manipulation, we propose a novel end-effector sampling method in the training period. It constructs a distance-invariant sampling sphere relative to the foot contact plane, which decouples end-effector goal from base pose and height variation, achieving stable and seamless end-effector tracking while traversing diverse terrains. Moreover, to mitigate catastrophic forgetting that the robot fails to perform whole-body motions after learning locomotion over diverse terrains, we develop a two-stage learning framework integrated with dual-policy distillation, where a cross-terrain locomotion controller and a whole-body controller on quasi-level plane will simultaneously supervise TA-WBC during training. Compared to the decoupled controller and the conventional blind WBC, TA-WBC demonstrates superior performance by traversing complex terrains while mitigating unexpected foot-end collisions, thereby achieving both high terrain adaptability and precise

end-effector tracking.

The main contributions are summarized as follows:

- We propose TA-WBC, a unified terrain-aware whole-body controller for the legged manipulator. With a hybrid exteroception encoder for explicit terrain features extraction, it achieves robust loco-manipulation and coordinated whole-body motion across diverse terrains.
- We propose a novel end-effector sampling approach tailored to cross-terrain loco-manipulation training. Through a sampling sphere above the foot contact plane, it decouples the end-effector goal from the fluctuations of base pose and height.
- To avoid catastrophic forgetting, we develop a two-stage learning framework integrated with dual-policy distillation, allowing the legged manipulator to possess whole-body coordination and perceptive traversal capability simultaneously.
- We validate our policy via extensive simulation and real-world experiments. It remarkably expands the reachable workspace, reduces the unexpected collision, and improves end-effector tracking accuracy of cross-terrain loco-manipulation.

II. RELATED WORK

A. Learning-based Legged Locomotion

Traditional model-based methods for legged locomotion [15], [16] with MPC exhibit high stability in structured environments. However, their robustness is severely bottlenecked when facing unmodeled external disturbances. To address this limitation, data-driven methods with deep reinforcement learning are becoming the mainstream solution. It primarily diverges into two directions: one that relies solely on proprioception, and another that incorporates perceptive input. The former, also known as the blind locomotion policy, depends exclusively on proprioceptive feedback to navigate the environment, which adapts through collision responses and variations in posture [17], [18] or implicit terrain imagination [19]. This approach demonstrates strong robustness on mildly uneven terrains, but the absence of exteroceptive perception presents inherent limitations. The degradation of control precision caused by physical collisions is unacceptable for delicate tasks, and the lack of prospective prediction makes the robot highly susceptible to being trapped in hazardous terrains that exceed its traversal capabilities. Consequently, perception-based locomotion control has emerged as another vital research direction. A series of works [20], [21] utilize depth images to detect the elevation platform or overhanging obstacles, enabling the robots to autonomously climb, crouch, and pass underneath. Elevation maps [22], [23], [24] can continuously reconstruct the 2.5D representation of the surroundings, exhibiting superior robustness in multi-directional, complex movements.

Although the robustness of legged locomotion has been remarkably improved, existing works only focus on traversing complex terrains, ignoring the whole-body loco-manipulation potential of legged manipulators, thereby restricting the practical applications in human-centric environments.

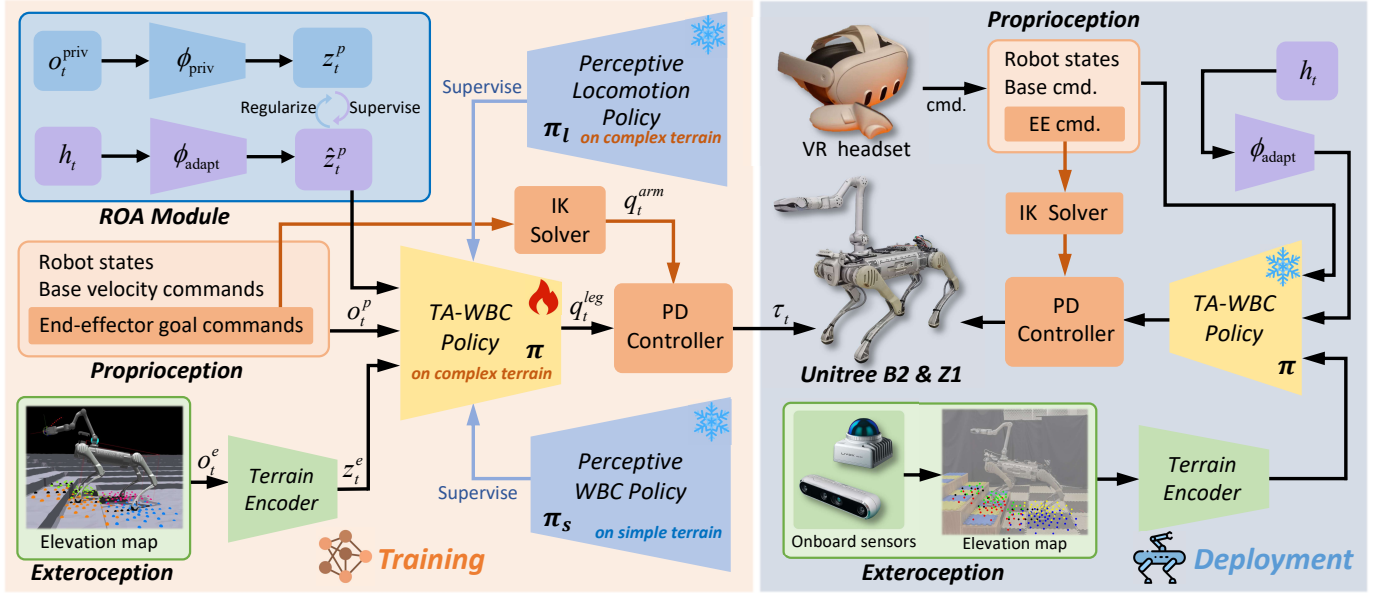


Fig. 2: Overview of the TA-WBC framework. TA-WBC is a unified perceptive whole-body controller over complex terrains. First, we train a perceptive whole-body policy π_s on quasi-level plane, and a perceptive locomotion policy π_l on complex terrains with randomly sampled joint configuration. After that, with the supervision of these two policies, TA-WBC is trained to maintain both the terrain traversability of π_l and the whole-body coordination motion of π_s over various terrains. The base and arm commands are sampled uniformly in training stage, while in deployment they are obtained by the VR headset.

B. Legged Loco-Manipulation

Coordinated legged loco-manipulation is challenging for high-dimensional joint states and deep coupling between the floating base and the onboard robotic arm. Rather than the decoupled control frameworks, unified architectures are becoming the mainstream method to solve this problem. The majority of traditional studies still relied on MPC and hierarchical QP to implement WBC for legged manipulators [25], [6], [26], [27], [28]. While MPC-based methods perform well in specific tasks, they lack sufficient generalization and robustness against external disturbances. To address this, Deep-WBC [4] introduces an RL-based approach by an advantage mixing module. Since then, a series of RL-based WBC frameworks have emerged: by integrating visual information, VBC [12] and UMI on Legs [29] enable legged manipulators to execute tasks autonomously; WBC capable of force control are proposed in [30] [31]; RoboDuet [5] and ReLIC [32] achieves whole-body coordination where the lower body actively assists the robotic arm; and a controller tailored for interactive navigation is developed in [33]. However, most existing whole-body controllers for legged manipulators still lack terrain perception. Although PILOT [13] achieves perceptive cross-terrain loco-manipulation for humanoid robots, perceptive WBC remains challenging for quadrupedal legged manipulators.

III. METHODOLOGY

In loco-manipulation tasks within complex and uneven environments, the primary challenge for legged manipulators lies in mastering high-dimensional control dynamics while simultaneously ensuring the robustness of end-effector tracking. To address these requirements, we propose TA-WBC, a unified end-to-end reinforcement learning framework tailored for loco-manipulation across various terrains, with the overview shown in 2. In this section, first, we establish the problem

definition, providing a rigorous definition of the state and action spaces. Next, we detail the core components in TA-WBC policy learning framework, highlighting the key modules that enable terrain-aware loco-manipulation.

A. Problem Definition

1) *State Space Design*: The state space \mathcal{S} is composed of two parts: the proprioceptive observation o_t^p and the perceptive observation o_t^e . Specifically, the proprioceptive observation is defined as:

$$o_t^p = [s_t^{\text{base}}, q_t, \dot{q}_t, a_{t-1}, c_t, s_t^{\text{foot}}, g_t, \hat{z}_t^p]. \quad (1)$$

Among them, there are base states $s_t^{\text{base}} \in \mathbb{R}^5$ including roll, pitch, and base angular velocities, joint positions $q_t \in \mathbb{R}^{18}$, joint velocities $\dot{q}_t \in \mathbb{R}^{18}$, and the last action of the policy $a_{t-1} \in \mathbb{R}^{12}$. Besides, the current commands $c_t = [v_t^{\text{base}_d}, \omega_t^{\text{base}_d}, p_t^{\text{arm}_d}]$, denoting desired base linear and angular velocities, and desired end-effector pose in the arm frame respectively. $s_t^{\text{foot}} \in \{0, 1\}^4$ denotes the foot contact state, where 1 indicates contact and 0 indicates swing phase. Inspired by [34], [17], we design $g_t \in \mathbb{R}^5$ to provide gait timing reference as a part of observation for a more stable walking pattern. Lastly, $\hat{z}_t^p \in \mathbb{R}^{20}$ represents the environment extrinsic physics, which is predicted by an adaptation encoder from a history of proprioceptive observations.

The exteroceptive observation $o_t^e \in \mathbb{R}^{50 \times 4}$ corresponds to an elevation map around the legged robot. Following the work of [35], first, we build a 2.5D robot-centric map from pointcloud perception, then sample an equal amount of points around every foot.

In conclusion, the complete observation of the policy is:

$$o_t = [o_{t-H}^p, o_{t-H+1}^p, \dots, o_{t-1}^p, o_t^p, o_t^e], \quad (2)$$

where $H = 10$ is the history horizon.

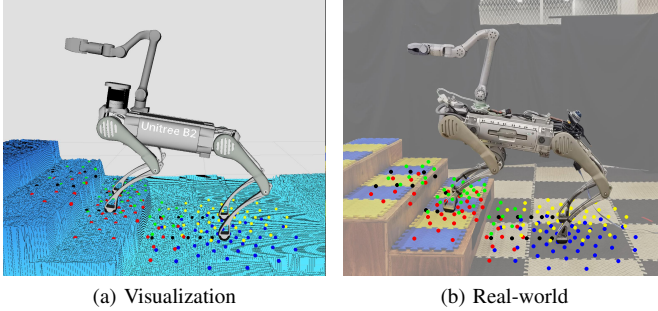


Fig. 3: Details of height sampling points for exteroceptive observation o_t^e in real-world experiment. Samples in different colors correspond to different feet, and samples in direction of $\theta = 0$ is represented by black points.

2) *Action Space Design*: Our controller is capable of controlling the legged robot and the mounted arm simultaneously. For the legged robot, the RL policy outputs the desired joint position for all 12 leg joints $q_t^{\text{leg}d}$, which is converted to torque command by a PD controller. The desired position of arm joints $q_t^{\text{arm}d}$ would be provided by the inverse kinematic (IK) method, which means the policy is trained to adjust its legs for an appropriate base pose for the end-effector to reach the target. Details about arm control can be found in Section III-B5.

B. Policy Learning

As shown in Fig. 2, TA-WBC receives proprioceptive observation o_t^p , exteroceptive latent z_t^e , and the latent environmental dynamics \hat{z}_t^p inferred from the proprioceptive history h_t . During training, two different policies will together supervise the output of TA-WBC, simultaneously enabling robust cross-terrain locomotion and expansive whole-body motion with a unified policy π . In this section, we will detail the critical modules in policy learning.

1) *Regularized Online Adaptation*: To achieve partially observable whole-body control, we utilize the regularized online adaptation (ROA) [4] framework consisting of a single actor-critic network and two complementary encoders. The privileged encoder ϕ_{priv} extracts a physics latent vector z_t^p from the privileged information o_t^{priv} , including actual friction, external payload, and motor strength. Simultaneously, an adaptation encoder ϕ_{adapt} is trained to implicitly infer latent environmental dynamics \hat{z}_t^p from the proprioceptive history h_t by imitating z_t^p , where $h_t = [o_{t-H}^p, o_{t-H+1}^p, \dots, o_{t-1}^p]$, $H = 10$. Additionally, the physics latent vector z_t^p is regularized to avoid large deviation from \hat{z}_t^p .

2) *Hybrid Exteroceptive Encoder*: Conventional terrain encoder typically relies on base-centric height grip maps, where elevation samples are collected in the base frame. However, this representation suffers from significant spatial misalignment; as the robot maneuvers, the relative transformation between the base-anchored grid and the swing foot remains highly dynamic, often resulting in insufficient perceptive resolution around the feet, which is critical to avoid unexpected collision during traversing terrains. Additionally, this design is always high-dimensional and coupled with an expansive flat MLP, leading to numerical instability or training divergence.

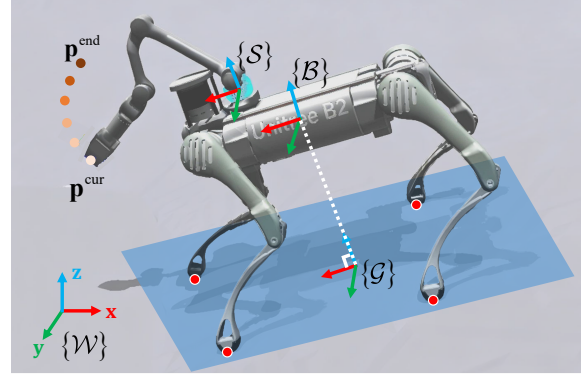


Fig. 4: Details of the construction of the FCP and the sampling sphere coordinate. The foot contact points are colored in red, and the FCP is represented by a blue plane.

To overcome this limitation, our approach utilizes a foot-centric, multi-ring sampling strategy, with a hybrid exteroceptive encoder tailored to this circular geometry. As shown in Fig. 3, for each foot $k \in \{1, 2, 3, 4\}$, we sample the terrain heights at $N_k = 50$ points arranged in $M = 5$ concentric rings centered at the foot's vertical projection. The samples are distributed along multiple concentric circles surrounding each foot, with radii $r = \{0.07, 0.14, 0.21, 0.30, 0.42\}$ m, containing $n = \{6, 8, 10, 12, 14\}$ points respectively. They are distributed along the angular dimension from $\theta \in [0, 2\pi)$, where the direction of $\theta = 0$ is aligned with the forward heading of the quadruped base in the horizontal plane.

This non-uniform density provides higher resolution around each foot and decouples the exteroception input from the base coordinate frame, enhancing collision-free locomotion over discrete terrains. Moreover, to leverage the structured sampling pattern from this method, the encoder adopts a hierarchical structure. Specifically, a 1D convolutional layers with circular padding first process each concentric ring independently. Subsequently, the local features M_k^f for each foot k are flattened and concatenated into a single vector $f_k \in \mathbb{R}^{\sum n_i \times n_c}$, where $\sum n_i = 50$ and $n_c = 4$ denote the number of convolution output channels. This combined feature vector f_k is then processed by an MLP to produce a compact latent vector $z_k^e \in \mathbb{R}^{20}$ for each foot. With the same encoder network shared across all four feet, the final exteroceptive latent vector $z^e = [z_1^e, z_2^e, z_3^e, z_4^e] \in \mathbb{R}^{80}$ is constructed.

This hybrid and hierarchical encoder can enhance training efficiency by explicitly exploiting the periodic nature of the circular sampling pattern, and also exploit the inherent morphological symmetry of the quadruped robot to reduce the parameter volume, resulting in rapid convergence.

3) *End-Effector Goal Sampling*: Previous works about legged loco-manipulation mostly assume a flat plane, always uniformly sampling target end-effector pose in a sphere coordinate system, where the origin's height with respect to the ground remains invariant [12]. This method ensures the consistency of trajectory, but is completely ineffective over non-planar terrain due to the continuous variation in base height and pose, especially pronounced changes in pitch. While [14] spherical end-effector pose sampling on uneven terrain, it is restricted to a static base configuration, consider-

ing environmental and self-collision constraints solely, which is unavailable to maintain continuous and stable goal samples during loco-manipulation.

Furthermore, to facilitate end-effector tracking accuracy in cross-terrain loco-manipulation, we propose a novel end-effector sampling method in training period. It constructs a distance-invariant sampling sphere relative to the foot contact plane, which decouples end-effector goal from base pose and height variation, achieving stable and seamless end-effector tracking while traversing diverse terrains.

To achieve seamless end-effector goal transition in cross-terrain loco-manipulation, we introduce a spherical sampling method based on the foot contact plane (FCP). Specifically, we construct the spherical sampling coordinate system \mathcal{S} which is distance-invariant relative to the FCP. As shown in Fig. 4, this plane is determined by the four foot contact points via least-squares fitting, and updated only upon detection of valid foot-ground contacts of all the feet, which is defined by a vertical contact force that is markedly greater than the horizontal components. The FCP is represented by its unit normal vector $\mathbf{n}_f \in \mathbb{R}^3$ and offset parameter $d_f \in \mathbb{R}$, subject to $\|\mathbf{n}_f\| = 1$ and the plane equation $\mathbf{n}_f \cdot \mathbf{x} + d_f = 0$.

Specifically, we define \mathcal{W} as the world frame, and \mathcal{B} as the base frame. Then, the base position \mathbf{p}_b is projected onto FCP along its normal vector \mathbf{n}_f for a ground projection point \mathbf{p}_G , and the x -axis of \mathcal{B} is projected onto the terrain plane:

$$\mathbf{v}_{\text{proj}} = \mathbf{x}_B - (\mathbf{x}_B \cdot \mathbf{n}_f)\mathbf{n}_f. \quad (3)$$

Then we construct the ground projection frame \mathcal{G} , with its origin located at \mathbf{p}_G , and its rotation matrix $\mathbf{R}_G = [\mathbf{x}_G, \mathbf{y}_G, \mathbf{z}_G] \in SO(3)$ is defined as:

$$\mathbf{z}_G = \mathbf{n}_f, \mathbf{x}_G = \frac{\mathbf{v}_{\text{proj}}}{\|\mathbf{v}_{\text{proj}}\|}, \mathbf{y}_G = \mathbf{z}_G \times \mathbf{x}_G. \quad (4)$$

Finally, the origin of sampling frame \mathcal{S} is obtained by applying a fixed offset \mathbf{p}_c in frame \mathcal{G} , and the three axes of \mathcal{S} are identical to those of \mathcal{G} . Subsequently, the final end-effector goal \mathbf{p}^{end} for each time interval of T_i is obtained by uniformly sampling within a sphere of radius $r_s = 0.8\text{m}$ centered at the origin of frame \mathcal{S} . Inspired by [12], we interpolate the end-effector goal command $\mathbf{p}_t^{\text{cmd}}$ between \mathbf{p}^{end} and end-effector current state \mathbf{p}^{cur} at intervals of T_i :

$$\mathbf{p}_t^{\text{cmd}} = \frac{t}{T_i}\mathbf{p}^{\text{cur}} + \left(1 - \frac{t}{T_i}\right)\mathbf{p}^{\text{end}}, \quad t \in [0, T_i]. \quad (5)$$

Through the above transformation, the sampled pitch and yaw angles become intrinsic to the valid foot contact plane. With additional collision check of terrain and base trunk, this sampling method achieves smooth and adaptive end-effector goal 6D pose sampling over different unstructured terrains, which significantly improves training efficiency.

4) *Policy Distillation*: To ensure the robot can perform collision-free loco-manipulation across various terrains, while simultaneously actuating whole-body joints to expand end-effector’s workspace, we employ a two-stage training method supervised by two distinct policies.

In the first stage, we train a perceptive policy π_s on simple terrain, achieving whole-body loco-manipulation on quasi-

TABLE I: REWARD DESIGN

Term	Weight	Term	Weight	Term	Weight
$r_{\omega_d}^{\text{base}}$	2.0	$r_{v_d}^{\text{base}}$	1.5	$r_{p_d}^{\text{arm}}$	1.8
$r_{\text{height}}^{\text{base}}$	-5.0	$r_{\text{pitch}}^{\text{base}}$	-0.1	$r_{\text{hip}}^{\text{base}}$	-0.8
$r_{\text{height}}^{\text{feet}}$	-4.5	$r_{\text{drag}}^{\text{feet}}$	-0.25	$r_{\text{gait}}^{\text{feet}}$	-3.0
r_τ	-10^{-7}	r_{smooth}	-0.015	$r_{\text{limit}}^{\text{dof}}$	-1.5

level plane with perception input. Concurrently, we train a terrain-aware cross-terrain locomotion policy π_l with randomly sampled arm joint configurations. In the second stage, we relax the mixing ratio introduced in [4], continuing the training based on π_s without any reward scale modification. The unified policy π is trained under the supervision of both π_s and π_l using PPO, augmented with a terrain-conditioned distillation loss defined as:

$$\mathcal{L}_{\text{distill}} = \mathbb{E}_s [\mathbb{I}(s)D_{\text{KL}}(\pi_s \parallel \pi) + (1 - \mathbb{I}(s))D_{\text{KL}}(\pi_l \parallel \pi)], \quad (6)$$

where $\mathbb{I}(s)$ is an indicator function equal to 1 when on quasi-level planes or received standing command for base, otherwise equal to 0. D_{KL} represents the Kullback-Leibler divergence between the continuous action distributions of the respective expert and the unified student policy π . This loss is integrated into the standard PPO objective, seamlessly guiding π to inherit precise whole-body manipulation skills from π_s , while acquiring robust locomotion reflexes from π_l elsewhere.

5) *Arm Control*: According to [4], a whole-body RL policy is capable of tracking the end-effector position, but struggles in accurately controlling the orientation. Although a keypoint-based representation of orientation is used in [14] and [36] for better tracking, it would increase the dimension of the goal command and introduce additional reward functions, thus making training harder to converge. To train a more robust and lower-computational policy, we employ the damped least squares method to solve the inverse kinematics of the robot arm in the world frame, which enhances numerical stability near singularities compared to the standard pseudoinverse method.

6) *Reward Design and Domain Randomization*: As detailed in Table I, we formulate the reward r_t as a weighted sum of three components: command tracking rewards for accurately tracking c_t , base stability rewards that encourage stable base pose and gait pattern, and regularization items that encourage smooth motions. For sim-to-real transfer, we implement domain randomization by randomizing parameters about physical properties (e.g., mass, friction, and actuator strength).

IV. EXPERIMENTS

A. Experiment Setup

1) *Robot System Setup*: Our hardware platform comprises a Unitree B2 quadruped robot and a Unitree Z1 6-DoF robotic arm equipped with a 1-DoF gripper. To acquire a real-time robot-centric elevation map, a forward-facing Intel RealSense D455 depth camera and a rear-mounted Livox Mid-360 LiDAR are mounted on the B2 torso.

TABLE II: SIMULATION RESULTS ON DIFFERENT TERRAINS. \uparrow : HIGHER IS BETTER; \downarrow : LOWER IS BETTER.

Terrain	Method	$V_w(m^3) \uparrow$	$l_{ter} \uparrow$	$E_v(m/s) \downarrow$	$E_{yaw}(rad/s) \downarrow$	$E_{ee}(m) \downarrow$	$r_c(\%) \downarrow$
(a) Simple	BL+IK	0.710	-	0.032	0.080	0.076	-
	Blind WBC	0.865	-	0.074	0.112	0.034	-
	TA-WBC (Ours)	0.884	-	0.059	0.131	0.025	-
(b) Complex	BL+IK	0.683	6.26	0.223	0.460	0.316	18.78
	PL+IK	0.683	9.00	0.082	0.227	0.155	0.97
	TA-WBC (Ours)	0.825	9.00	0.109	0.252	0.042	0.56

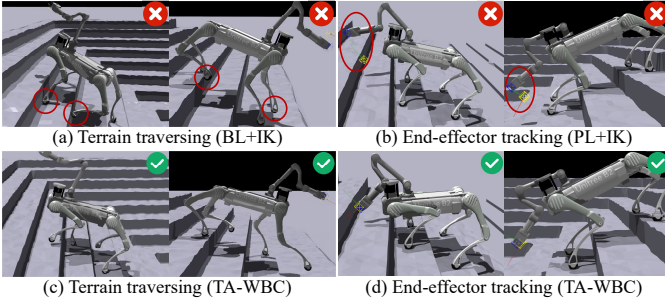


Fig. 5: Simulation results on various terrains compared with baselines.

2) *Evaluation Metrics*: To quantify the performance of the proposed method and baselines, we define the following metrics: (1) linear velocity tracking error (E_v): the difference between command and actual base linear velocity; (2) yaw rate tracking error (E_{yaw}): the difference between command and actual base yaw rate; (3) end-effector position tracking error (E_{ee}): the Euclidean distance between the target and actual end-effector position; (4) workspace (V_w): subtracted by the volume of the convex hull formed by 1000 reachable end-effector target positions. Specifically, a target position is considered reachable if the end-effector successfully reaches it within a predefined threshold of $E_{ee} \leq 0.03m$ without collision; (5) unexpected contact rate (r_c): the frequency of horizontal impacts or accidental slips occurring on the four feet during traversing complex terrains, especially on stairs; (6) maximum available terrain level (l_{ter}): the highest terrain level traversable by the robot. Traversability is defined as achieving a success rate exceeding 95% with $E_v \leq 0.1m/s$. $l_{ter} \in [0, 9]$, where 9 represents the maximum stair height, discrete step height, and slope inclination angles.

B. Simulation Results

1) *Comparison with Baselines*: We compare our method against baselines in both simple plane and complex non-flat scenarios with slopes, steps, and stairs.

Simple Terrain: We first verify the performance on simple quasi-horizontal terrain, which is approximately a level plane without significant irregularities. We compare TA-WBC against the following algorithms: (1) **Blind Locomotion and IK (BL+IK)**: a proprioception-based locomotion policy with a decoupled IK solver for the robotic arm; (2) **Blind Whole-Body Control (Blind WBC)**: a whole-body controller for legged manipulators with proprioception only, which is trained based on [12].

As the result shown in Table II(a), despite the remarkably increased input dimensionality from the additional terrain perception, TA-WBC maintains excellent performance similar to Blind WBC on flat ground. Additionally, our controller

outperforms the decoupled baseline (BL+IK) significantly in terms of V_w and E_{ee} , which stems from the coordinated motion of leg joints. Since the decoupled method treats the onboard arm as a payload, while TA-WBC is required to track base and end-effector commands simultaneously, the performance in E_v and E_{yaw} decrease. Nevertheless, this degradation is slight enough to be negligible compared with the considerable improvement in workspace and end-effector tracking, which is more critical for loco-manipulation tasks.

Complex Terrain: To verify the terrain adaptability and loco-manipulation capability of TA-WBC, we compare it against the following methods on complex terrains including quasi-plane, ascending and descending slopes, staircases, and discrete steps: (1) **Blind Locomotion and IK (BL+IK)**: a proprioception-based cross-terrain locomotion policy with a decoupled IK solver for the arm; (2) **Perceptive Locomotion and IK (PL+IK)**: a cross-terrain locomotion policy with both proprioception and exteroception, with a decoupled IK solver for the arm.

It is noteworthy that the performance of blind WBC over complex terrain is compared in Section IV-B2. As shown in Table III(b) and Fig. 5(a), the robot with BL+IK fails to lift its feet proactively before horizontal contact occurs, resulting in the highest r_c and the largest E_{ee} . The robot with PL+IK is able to anticipate terrain and avoid stumbles, however, as shown in Fig. 5(b), maintains a relatively fixed base pitch while traversing stairs and slopes, leading to a limited workspace (V_m). In contrast, TA-WBC not only enables collision-free locomotion (Fig. 5(c)) but also, when standing on slopes or stairs, allows the front legs to bend and achieves whole-body coordination (Fig. 5(d)), substantially expanding the reachable workspace.

2) *Ablation Study*: We perform ablation studies to validate the contribution of each module, as detailed in Table III. With a pure proprioceptive WBC over complex terrains, the robot is unable to perceive upcoming terrain and react in advance, resulting in the worst performance across all metrics, which validate the indispensable nature of exteroception. Furthermore, the sampling and encoding strategies for terrain exteroception are also crucial. By replacing foot-centric multi-ring sampling with a base-centric grip one, or employing a flat MLP rather than our hybrid architecture, the training convergence gets slower, l_{ter} decreases, and foot stumble r_c increases by at least 400%. Moreover, the removal of policy distillation module leads to gradient interference, significantly reducing V_w both on quasi-level plane and complex terrains. These results validate the contributions of individual components, revealing their effects in enhancing cross-terrain stability and expanding reachable workspace.

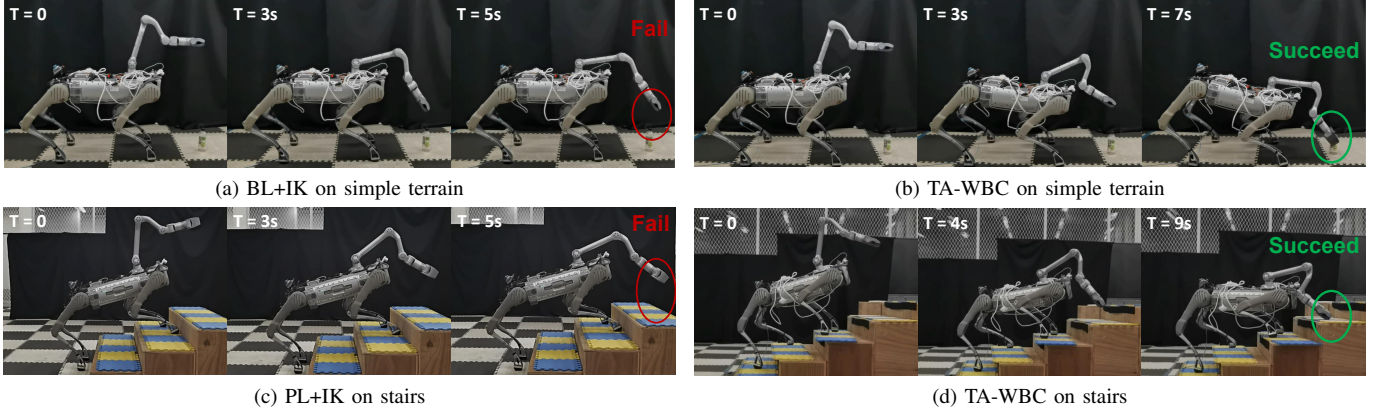


Fig. 6: Comparison between decoupled controller and TA-WBC when the end-effector goal reaches the ground.

TABLE III: ABLATION RESULTS OF KEY MODULES OVER COMPLEX TERRAINS.

Method	Exter.	Foot.	Hybrid Enc.	Distill.	$V_m(\text{m}^3) \uparrow$	$l_{\text{ter}} \uparrow$	$E_v(\text{m/s}) \downarrow$	$E_{y_{\text{aw}}}(\text{rad/s}) \downarrow$	$E_{\text{ee}}(\text{m}) \downarrow$	$r_c(\%) \downarrow$
(a)	✗	✗	✗	✗	0.766	5.57	0.205	0.431	0.289	24.37
(b)	✓	✗	✓	✓	0.814	8.76	0.127	0.309	0.070	2.57
(c)	✓	✓	✗	✓	0.809	8.20	0.126	0.274	0.103	4.20
(d)	✓	✓	✓	✗	0.742	8.73	0.118	0.365	0.161	0.88
TA-WBC (Ours)	✓	✓	✓	✓	0.825	9.00	0.109	0.252	0.042	0.56

Remark: (a) Removing all the exteroception input; (b) Replacing foot-centric elevation sampling with base-centric grip sampling; (c) Replacing hybrid terrain encoder with a flat MLP; (d) Removing policy distillation module.

C. Real-World Deployment

We directly deploy the trained policy in a real-world robot system via zero-shot transfer. The whole-body actor outputs the target joint positions for leg joints at 50 Hz, which are subsequently transmitted to low-level PD controllers for motors that run at 500 Hz. For the acquisition of real-time foot-centric terrain perception, we utilize the onboard depth camera and LiDAR to construct the elevation map with the framework in [37]. For convenience, the high-level commands consisting of the target end-effector pose, base linear velocity, and base angular velocity is obtained by VR teleoperation from a Meta Quest 3.

1) *Standing Whole-Body Motion:* As shown in Fig. 6(a), when the end-effector target pose is very low (even when reaching the ground), the legged manipulator with the decoupled policy fails to reach due to the original limitation of the robotic arm workspace. However, with TA-WBC shown in Fig. 6(b), the robot is able to adjust the base pitch and grasp the bottle on flat ground with a height less than 10 cm. Such coordination enables substantial base pitch adjustments to assist the robotic arm, thereby remarkably expanding the arm workspace. Furthermore, in the stair scenario, we manually stop the robot midway while ascending. As shown in Fig. 6(d), its hind left and right feet even stand on two different steps, leading to a non-zero roll and pitch base pose. Although it is challenging to keep balance in that case, our method still enables the end-effector to directly reach the ground, with a dynamic variation on pitch exceeding 25 degrees.

2) *Long-Horizon Loco-Manipulation:* To verify the terrain traversal capability of TA-WBC, we design a long-horizon cross-terrain loco-manipulation task shown in Fig. 7. Specifically, the robot is teleoperated to execute a series of tasks: first,

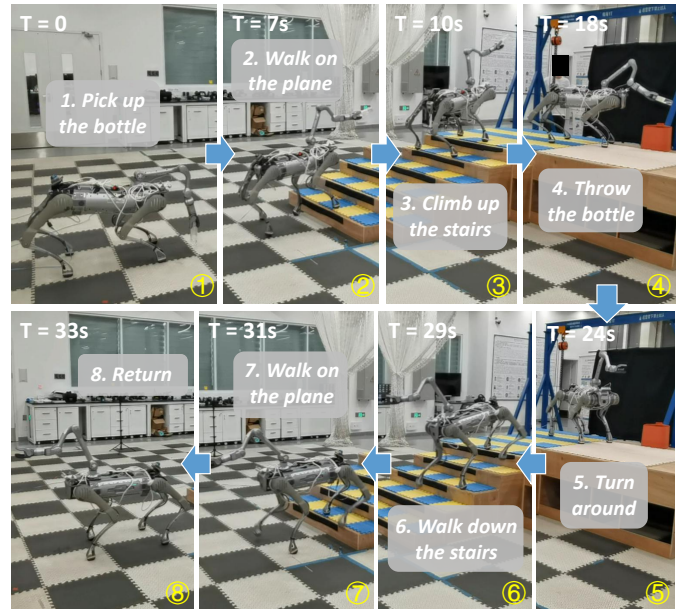


Fig. 7: Overview of the continuous long-horizon cross-terrain loco-manipulation task.

start from flat plane and pick up the bottle on the ground; then, climb up the stairs consisting of five steps with a height of 17 cm; after that, approach the trash bin placed on the platform and throw the bottle in; finally, turn around on the platform and walk downstairs, returning to the starting zone.

In this real-world case, our method enables the robot to walk on stairs at a speed of up to 0.8 m/s without any unexpected collision between feet and terrain, demonstrating strong flexibility and high security. Furthermore, in order to validate the robustness and adaptability of our proposed

method, we repeatedly restart and test by setting different starting zones, diverse grasping targets, and various velocity commands. The result shows that the legged manipulator with TA-WBC can successfully finish this long-horizon challenging task 5 times in a row without any falls or stumbles, verifying the robustness of our framework.

V. CONCLUSION

In this paper, we propose TA-WBC, a terrain-aware unified end-to-end RL framework for legged loco-manipulation over various terrains. With elevation sampling points around feet as perception input, and assistance of policy distillation, TA-WBC first achieves expansive and cross-terrain whole-body control with one single controller. Simulation and real-world deployment validate its robustness on terrain traversability and expanding end-effector tracking, showing the potential of long-horizon outdoor legged loco-manipulation tasks. Future works include the development of sophisticated high-level policies that seamlessly integrate with TA-WBC as the robust low-level controller, which is expected to enable the legged manipulators to achieve fully autonomous loco-manipulation task execution over various terrains.

REFERENCES

- [1] Z. Fu, T. Z. Zhao, and C. Finn, "Mobile aloha: Learning bimanual mobile manipulation with low-cost whole-body teleoperation," *arXiv preprint arXiv:2401.02117*, 2024.
- [2] C. Wu, R. Wang, Y. Zeng, J. Wang, M. Zhang, G. Zheng, Q. Niu, J. Zheng, J. Ma, and B. Zhou, "Synergizing efficiency and reliability for continuous mobile manipulation," *arXiv preprint arXiv:2604.05430*, 2026.
- [3] M. V. Minniti, F. Farshidian, R. Grandia, and M. Hutter, "Whole-body mpc for a dynamically stable mobile manipulator," *IEEE Robotics and Automation Letters*, vol. 4, no. 4, pp. 3687–3694, 2019.
- [4] Z. Fu, X. Cheng, and D. Pathak, "Deep whole-body control: learning a unified policy for manipulation and locomotion," in *Conference on Robot Learning*. PMLR, 2023, pp. 138–149.
- [5] G. Pan, Q. Ben, Z. Yuan, G. Jiang, Y. Ji, S. Li, J. Pang, H. Liu, and H. Xu, "Roboduet: Learning a cooperative policy for whole-body legged loco-manipulation," *IEEE Robotics and Automation Letters*, 2025.
- [6] L. Molnar, J. Cheng, G. Fadini, D. Kang, F. Zargarbashi, and S. Coros, "Whole-body inverse dynamics mpc for legged loco-manipulation," *IEEE Robotics and Automation Letters*, 2025.
- [7] A. Escande, N. Mansard, and P.-B. Wieber, "Hierarchical quadratic programming: Fast online humanoid-robot motion generation," *The International Journal of Robotics Research*, vol. 33, no. 7, pp. 1006–1028, 2014.
- [8] B. U. Rehman, M. Focchi, J. Lee, H. Dallali, D. G. Caldwell, and C. Semini, "Towards a multi-legged mobile manipulator," in *2016 IEEE International Conference on Robotics and Automation*. IEEE, 2016, pp. 3618–3624.
- [9] M. Zimmer, P. Viappiani, and P. Weng, "Teacher-student framework: a reinforcement learning approach," in *AAMAS Workshop Autonomous Robots and Multirobot Systems*, 2014.
- [10] M. Zhang, Y. Ma, T. Miki, and M. Hutter, "Learning to open and traverse doors with a legged manipulator," *arXiv preprint arXiv:2409.04882*, 2024.
- [11] K. Jiang, Z. Fu, J. Guo, W. Zhang, and H. Chen, "Learning whole-body loco-manipulation for omni-directional task space pose tracking with a wheeled-quadrupedal-manipulator," *IEEE Robotics and Automation Letters*, 2024.
- [12] M. Liu, Z. Chen, X. Cheng, Y. Ji, R.-Z. Qiu, R. Yang, and X. Wang, "Visual whole-body control for legged loco-manipulation," *arXiv preprint arXiv:2403.16967*, 2024.
- [13] X. Cui, L. Feng, Y. Zhou, H. Han, Z. Liu, and H. Wang, "Pilot: A perceptive integrated low-level controller for loco-manipulation over unstructured scenes," *arXiv preprint arXiv:2601.17440*, 2026.
- [14] T. Portela, A. Cramariuc, M. Mittal, and M. Hutter, "Whole-body end-effector pose tracking," in *2025 IEEE International Conference on Robotics and Automation*. IEEE, 2025, pp. 11 205–11 211.
- [15] P. M. Wensing, M. Posa, Y. Hu, A. Escande, N. Mansard, and A. Del Prete, "Optimization-based control for dynamic legged robots," *IEEE Transactions on Robotics*, vol. 40, pp. 43–63, 2023.
- [16] J. Di Carlo, P. M. Wensing, B. Katz, G. Bledt, and S. Kim, "Dynamic locomotion in the mit cheetah 3 through convex model-predictive control," in *2018 IEEE/RSJ International Conference on Intelligent Robots and Systems*. IEEE, 2018, pp. 1–9.
- [17] G. B. Margolis and P. Agrawal, "Walk these ways: Tuning robot control for generalization with multiplicity of behavior," in *Conference on Robot Learning*. PMLR, 2023, pp. 22–31.
- [18] N. Rudin, D. Hoeller, P. Reist, and M. Hutter, "Learning to walk in minutes using massively parallel deep reinforcement learning," in *Conference on Robot Learning*. PMLR, 2022, pp. 91–100.
- [19] I. M. A. Nahrendra, B. Yu, and H. Myung, "Dreamwaq: Learning robust quadrupedal locomotion with implicit terrain imagination via deep reinforcement learning," in *2023 IEEE International Conference on Robotics and Automation*. IEEE, 2023, pp. 5078–5084.
- [20] X. Cheng, K. Shi, A. Agarwal, and D. Pathak, "Extreme parkour with legged robots," in *2024 IEEE International Conference on Robotics and Automation*. IEEE, 2024, pp. 11 443–11 450.
- [21] Z. Zhuang, Z. Fu, J. Wang, C. G. Atkeson, S. Schwertfeger, C. Finn, and H. Zhao, "Robot parkour learning," in *Conference on Robot Learning*. PMLR, 2023, pp. 73–92.
- [22] J. He, C. Zhang, F. Jenelten, R. Grandia, M. Bächer, and M. Hutter, "Attention-based map encoding for learning generalized legged locomotion," *Science Robotics*, vol. 10, no. 105, p. eadv3604, 2025.
- [23] J. Ren, T. Huang, H. Wang, Z. Wang, Q. Ben, J. Long, Y. Yang, J. Pang, and P. Luo, "Vb-com: Learning vision-blind composite humanoid locomotion against deficient perception," *arXiv preprint arXiv:2502.14814*, 2025.
- [24] H. Wang, Z. Wang, J. Ren, Q. Ben, T. Huang, W. Zhang, and J. Pang, "Beamdojo: Learning agile humanoid locomotion on sparse footholds," *arXiv preprint arXiv:2502.10363*, 2025.
- [25] S. Zimmermann, R. Poranne, and S. Coros, "Go fetch!-dynamic grasps using boston dynamics spot with external robotic arm," in *2021 IEEE International Conference on Robotics and Automation*. IEEE, 2021, pp. 4488–4494.
- [26] E. Arcari, M. V. Minniti, A. Scampicchio, A. Carron, F. Farshidian, M. Hutter, and M. N. Zeilinger, "Bayesian multi-task learning mpc for robotic mobile manipulation," *IEEE Robotics and Automation Letters*, vol. 8, no. 6, pp. 3222–3229, 2023.
- [27] J.-R. Chiu, J.-P. Sleiman, M. Mittal, F. Farshidian, and M. Hutter, "A collision-free mpc for whole-body dynamic locomotion and manipulation," in *2022 International Conference on Robotics and Automation*. IEEE, 2022, pp. 4686–4693.
- [28] C. D. Bellicoso, K. Krämer, M. Stäuble, D. Sako, F. Jenelten, M. Bjelonic, and M. Hutter, "Alma-articulated locomotion and manipulation for a torque-controllable robot," in *2019 International Conference on Robotics and Automation*. IEEE, 2019, pp. 8477–8483.
- [29] H. Ha, Y. Gao, Z. Fu, J. Tan, and S. Song, "Umi-on-legs: Making manipulation policies mobile with manipulation-centric whole-body controllers," in *Conference on Robot Learning*. PMLR, 2025, pp. 5254–5270.
- [30] P. Zhi, P. Li, J. Yin, B. Jia, and S. Huang, "Learning a unified policy for position and force control in legged loco-manipulation," in *Conference on Robot Learning*. PMLR, 2025, pp. 652–669.
- [31] T. Portela, G. B. Margolis, Y. Ji, and P. Agrawal, "Learning force control for legged manipulation," in *2024 IEEE International Conference on Robotics and Automation*. IEEE, 2024, pp. 15 366–15 372.
- [32] X. Zhu, Y. Chen, L. Sun, F. Niroui, S. L. Cleac'h, J. Wang, and K. Fang, "Versatile loco-manipulation through flexible interlimb coordination," *arXiv preprint arXiv:2506.07876*, 2025.
- [33] Z. Bi, K. Chen, C. Zheng, Y. Li, H. Li, and J. Ma, "Interactive navigation for legged manipulators with learned arm-pushing controller," in *2025 IEEE/RSJ International Conference on Intelligent Robots and Systems*. IEEE, 2025, pp. 9–16.
- [34] A. Agarwal, A. Kumar, J. Malik, and D. Pathak, "Legged locomotion in challenging terrains using egocentric vision," in *Conference on Robot Learning*. PMLR, 2023, pp. 403–415.
- [35] T. Miki, J. Lee, J. Hwangbo, L. Wellhausen, V. Koltun, and M. Hutter, "Learning robust perceptive locomotion for quadrupedal robots in the wild," *Science Robotics*, vol. 7, no. 62, p. eabk2822, 2022.

- [36] A. Allshire, M. Mittal, V. Lodaya, V. Makoviychuk, D. Makoviichuk, F. Widmaier, M. Wüthrich, S. Bauer, A. Handa, and A. Garg, "Transferring dexterous manipulation from gpu simulation to a remote real-world trifinger," in *2022 IEEE/RSJ International Conference on Intelligent Robots and Systems*. IEEE, 2022, pp. 11 802–11 809.
- [37] T. Miki, L. Wellhausen, R. Grandia, F. Jenelten, T. Homberger, and M. Hutter, "Elevation mapping for locomotion and navigation using gpu," in *2022 IEEE/RSJ International Conference on Intelligent Robots and Systems*. IEEE, 2022, pp. 2273–2280.